Expanded View Figures

Figure EV1. Interaction of PSPs with SWI/SNF complex is not cell line dependent and persists post-nuclease treatment.

A Heat map of the ingenuity pathway analysis (IPA) of the enriched interactors identified in MudPIT analysis.
B Western blotting of purified ARID1B complexes from 293T, HeLa, and HCT116 nuclear extracts with paraspeckle components—PSPC1, SFPQ, and NONO. SMARCD1 was used as a positive control for purification.
C PSPC1 purified complexes were subjected to western with SWI/SNF antibodies—ARID1B and SMARCD1. The nuclear extracts were prepared post-72 h of transfection.
D Comparison of binding affinities of Halo-FLAG-ARID1B with PSPC1, SFPQ, and NONO with and without treatment of nuclear extract with salt active nuclease (SAN). Western blotting with SMARCD1 was used as a positive control.
E Comparison of the overall nuclei acid content and NEAT1 in the inputs used for the purification. GAPDH and 18 s rRNA were used as a control. An equal volume of extract was loaded and used for RNA extraction.

Source data are available online for this figure.

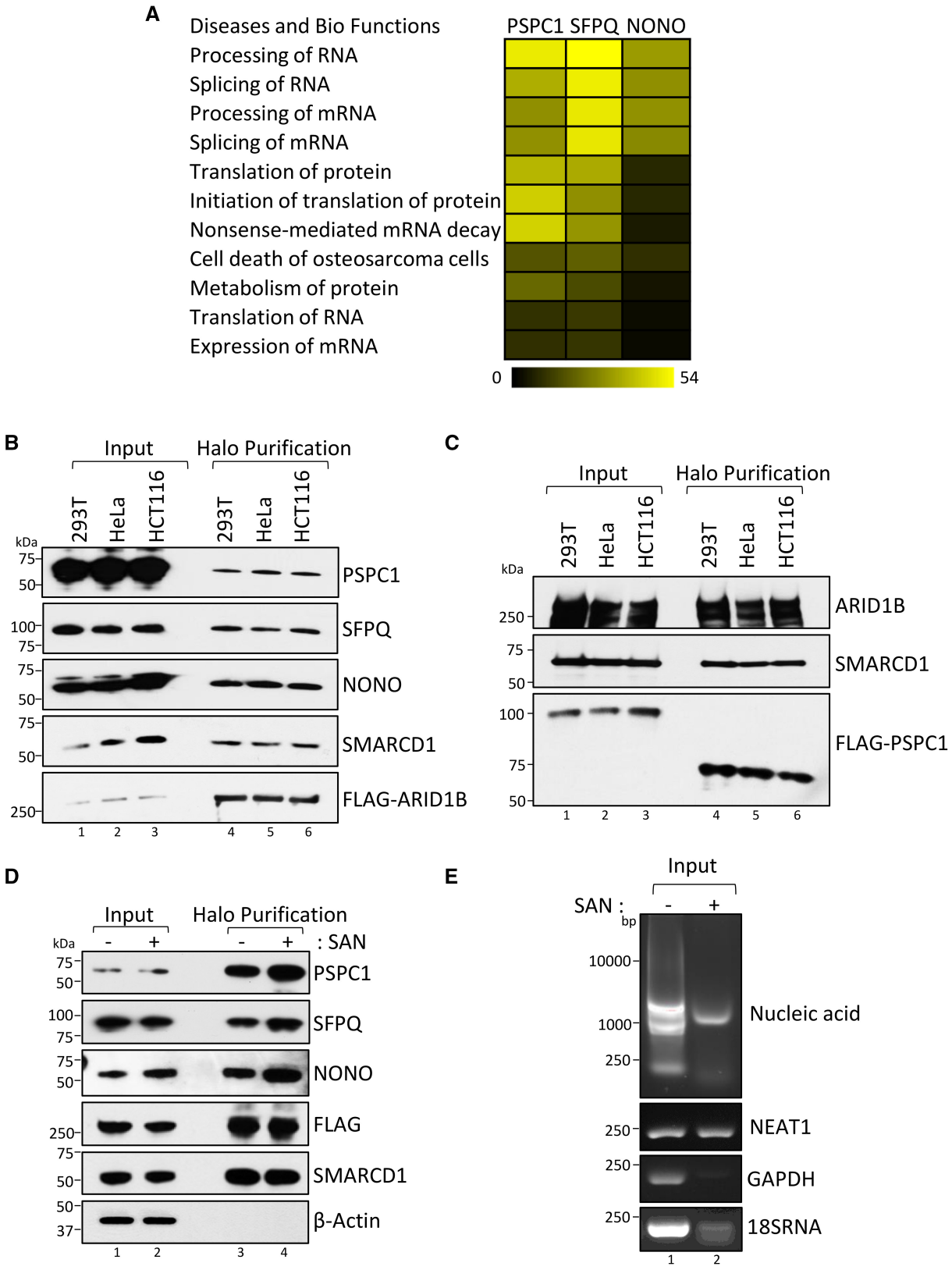
A
Diseases and Bio Functions
PSPC1 SFPQ NONO
Processing of RNA
Splicing of RNA
Processing of mRNA
Splicing of mRNA
Translation of protein
Initiation of translation of protein
Nonsense-mediated mRNA decay
Cell death of osteosarcoma cells
Metabolism of protein
Translation of RNA
Expression of mRNA
0
54
B
Input
Halo Purification
293T
HeLa
HCT116
293T
HeLa
HCT116
kDa
PSPC1
SFPQ
NONO
SMARCD1
FLAG-ARID1B
1 2 3 4 5 6
C
Input
Halo Purification
293T
HeLa
HCT116
293T
HeLa
HCT116
kDa
ARID1B
SMARCD1
FLAG-PSPC1
1 2 3 4 5 6
D
Input
Halo Purification
kDa
- + - + : SAN
PSPC1
SFPQ
NONO
FLAG
SMARCD1
β-Actin
1 2 3 4
E
Input
SAN : - +
bp
Nucleic acid
NEAT1
GAPDH
18SRNA
1 2

Figure EV1.

Figure EV2. Paraspeckle protein interactome is dependent on NEAT1 but not on ARID1B.

A RNA was isolated from HEK293FRT cells transfected with siRNA and RT–PCR was performed to check the transcript levels of total NEAT1 and its longer isoform NEAT1_2. Values were normalized to GAPDH expression. Error bars represent the standard error of two different biological experiments performed in technical duplicates (two-tailed *t*-test ****$P < 0.0001$)

B smFISH analysis performed to detect NEAT1 signal in the nucleus. The signal seen in the nucleus of the control cells was ensured as a specific signal and not an artifact by using a no-probe control, in which the cells were treated exactly as control; however, the NEAT1 probe was not added. The scale bar corresponds to 10 μm.

C Western blotting with various antibodies corresponding to SWI/SNF subunits to compare their expression upon NEAT1 knockdown with scramble-treated control. Beta-actin has been used as a loading control.

D Silver-stained gel image of the affinity-purified PSPC1, SFPQ, and NONO from NEAT1-depleted cells.

E Venn diagram showing the overlap between 685 common proteins identified in control and 347 proteins from NEAT1-depleted PSPC1, SFPQ, and NONO purifications.

F Western blotting for showing the specificity of ARID1B depletion using ARID1B-stable knockdown HEK293FRT cells. Beta-actin was used as a loading control.

G Silver-stained gel image of the affinity-purified SFPQ and NONO in ARID1B-depleted cells.

Source data are available online for this figure.

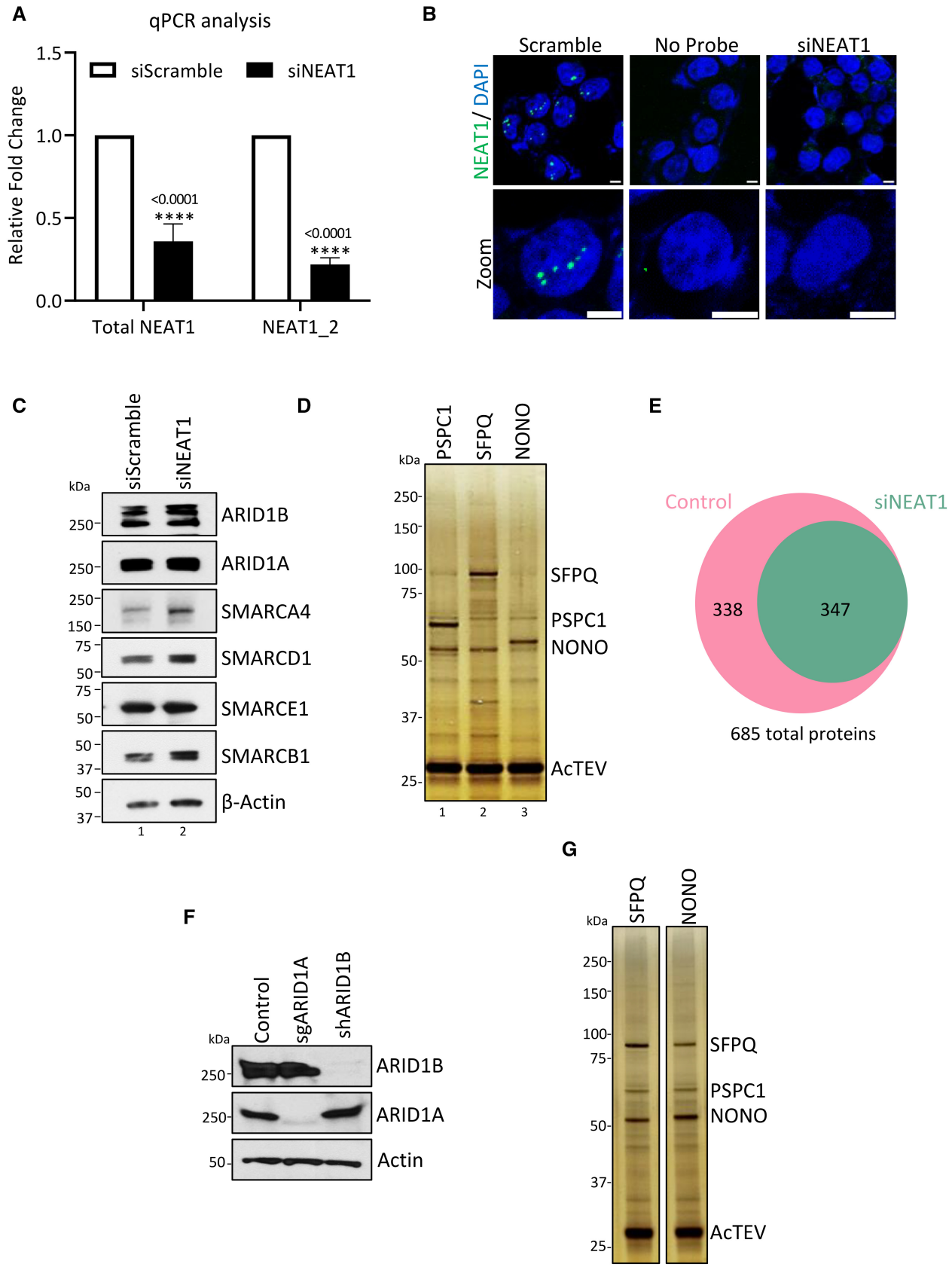
A
qPCR analysis
siScramble
siNEAT1
Relative Fold Change
1.5
1.0
0.5
0.0
<0.0001
****
<0.0001
****
Total NEAT1
NEAT1_2
B
Scramble
No Probe
siNEAT1
NEAT1/ DAPI
Zoom
C
siScramble
siNEAT1
kDa
ARID1B
ARID1A
SMARCA4
SMARCD1
SMARCE1
SMARCB1
β-Actin
D
PSPC1
SFPQ
NONO
kDa
SFPQ
PSPC1
NONO
AcTEV
E
Control
siNEAT1
338
347
685 total proteins
F
Control
sgARID1A
shARID1B
kDa
ARID1B
ARID1A
Actin
G
SFPQ
NONO
kDa
SFPQ
PSPC1
NONO
AcTEV

Figure EV2.

Figure EV3. Depletion of ARID1 paralogs leads to non-redundant transcriptional outcomes.

A Graph showing the decrease in expression of ARID1A and ARID1B in RNA-seq analysis post-siRNA treatment.

B, C Volcano plots for ARID1A and ARID1B show the proportion of up- and downregulated genes. Specific numbers are marked.

D, E Venn diagram depicting the overlap between (D) differentially expressed genes and (E) AS events. SE, skipped exon; A5SS, alternate 5′ splice site; A3SS, alternate 3′ splice site; MXE, mutually exclusive exon; RI, retained intron.

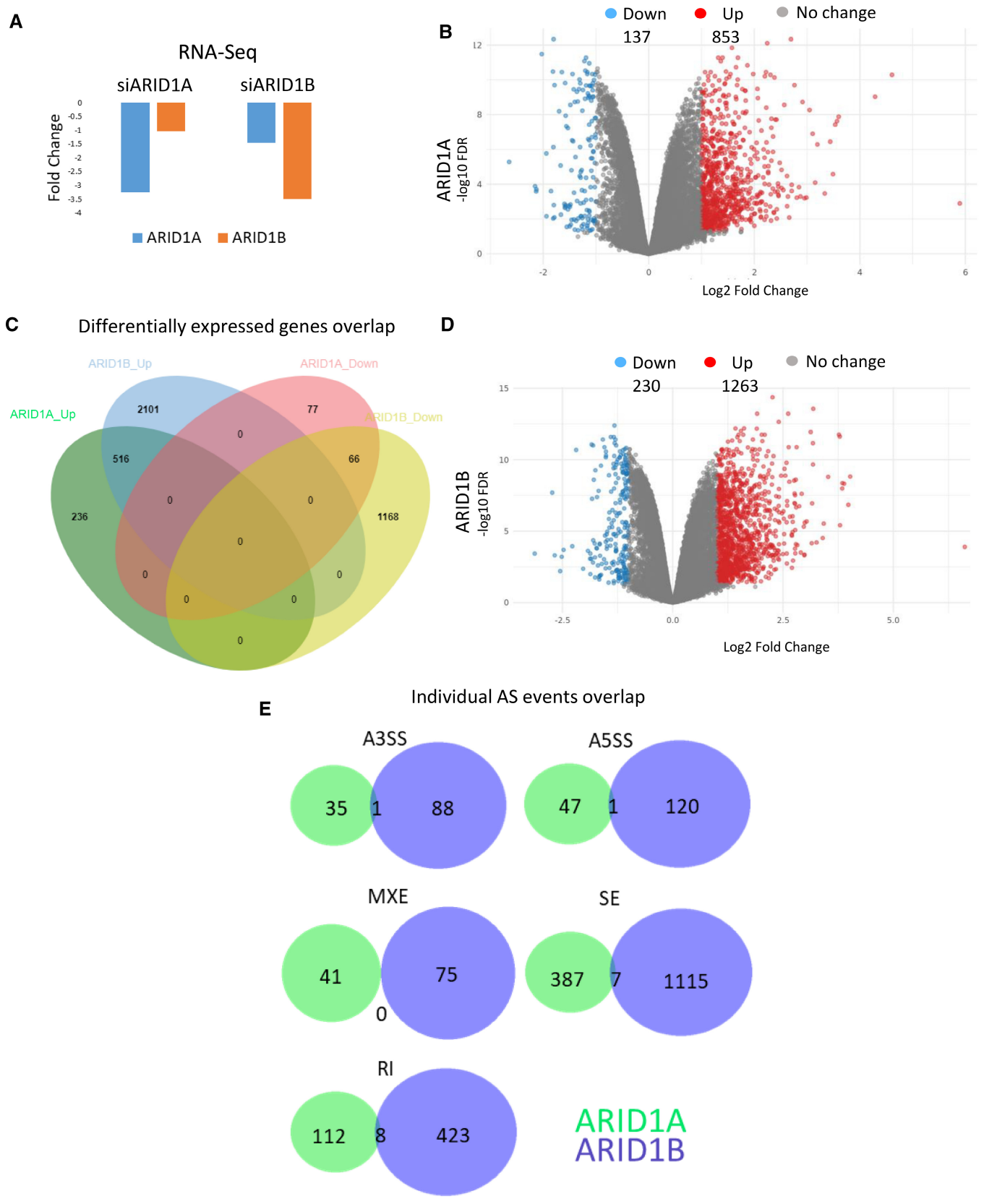
A
RNA-Seq
siARID1A
siARID1B
Fold Change
ARID1A
ARID1B
B
Down
Up
No change
137
853
ARID1A
-log10 FDR
Log2 Fold Change
C
Differentially expressed genes overlap
ARID1B_Up
ARID1A_Down
ARID1A_Up
ARID1B_Down
2101
77
516
66
236
1168
D
Down
Up
No change
230
1263
ARID1B
-log10 FDR
Log2 Fold Change
E
Individual AS events overlap
A3SS
35
1
88
A5SS
47
1
120
MXE
41
75
0
SE
387
7
1115
RI
112
8
423
ARID1A
ARID1B

Figure EV3.

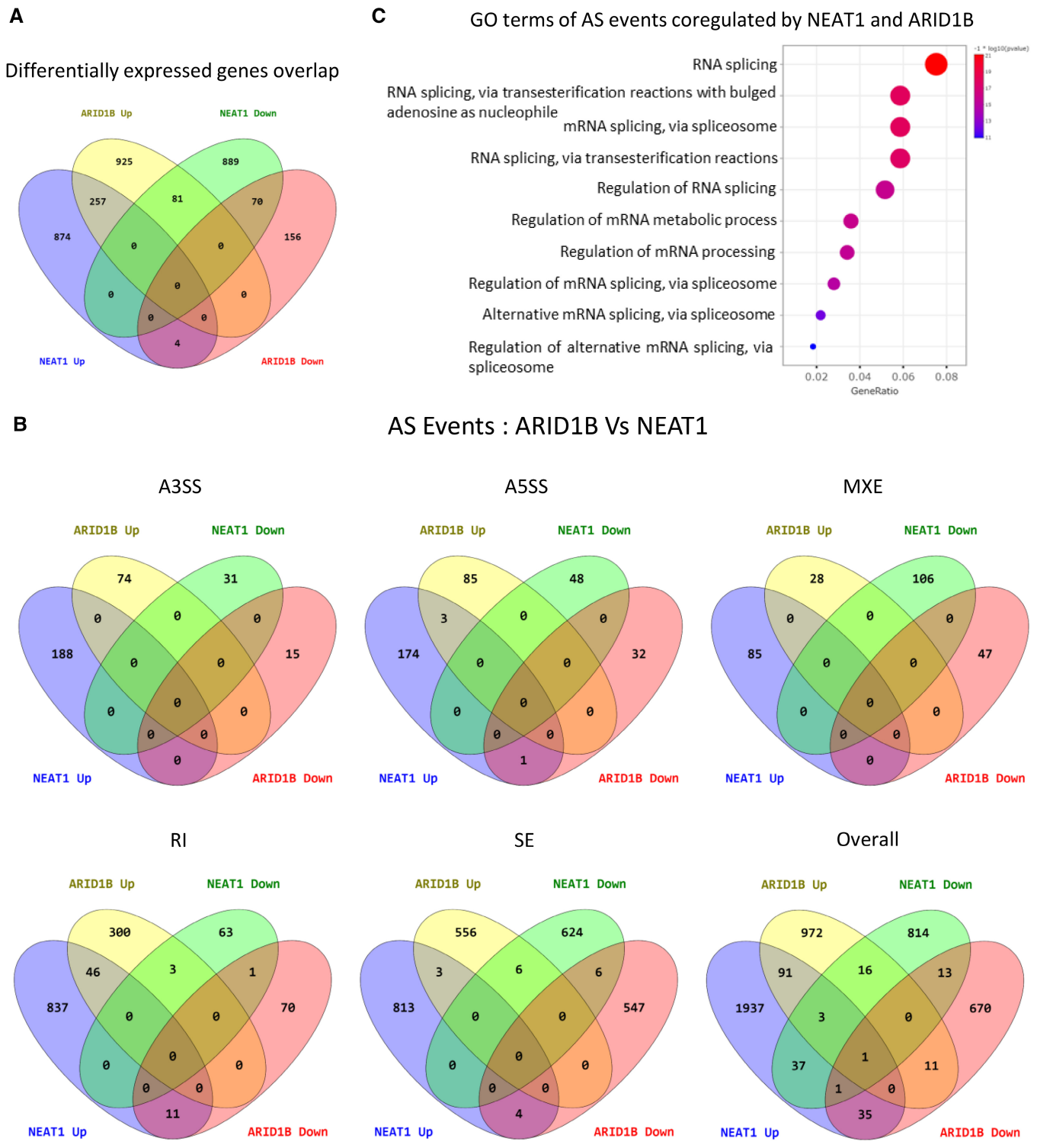

Figure EV4. NEAT1 and ARID1B depletions regulate similar transcription and AS of a few genes.

A, B Venn diagram showing the overlap of (A) differential expression of genes and (B) AS events upon ARID1B and NEAT1 depletion. SE, skipped exon; A5SS, alternate 5′ splice site; A3SS, alternate 3′ splice site; MXE, mutually exclusive exon; RI, retained intron.

C GO analysis of the alternatively spliced genes specifically observed post-depletion of ARID1B.

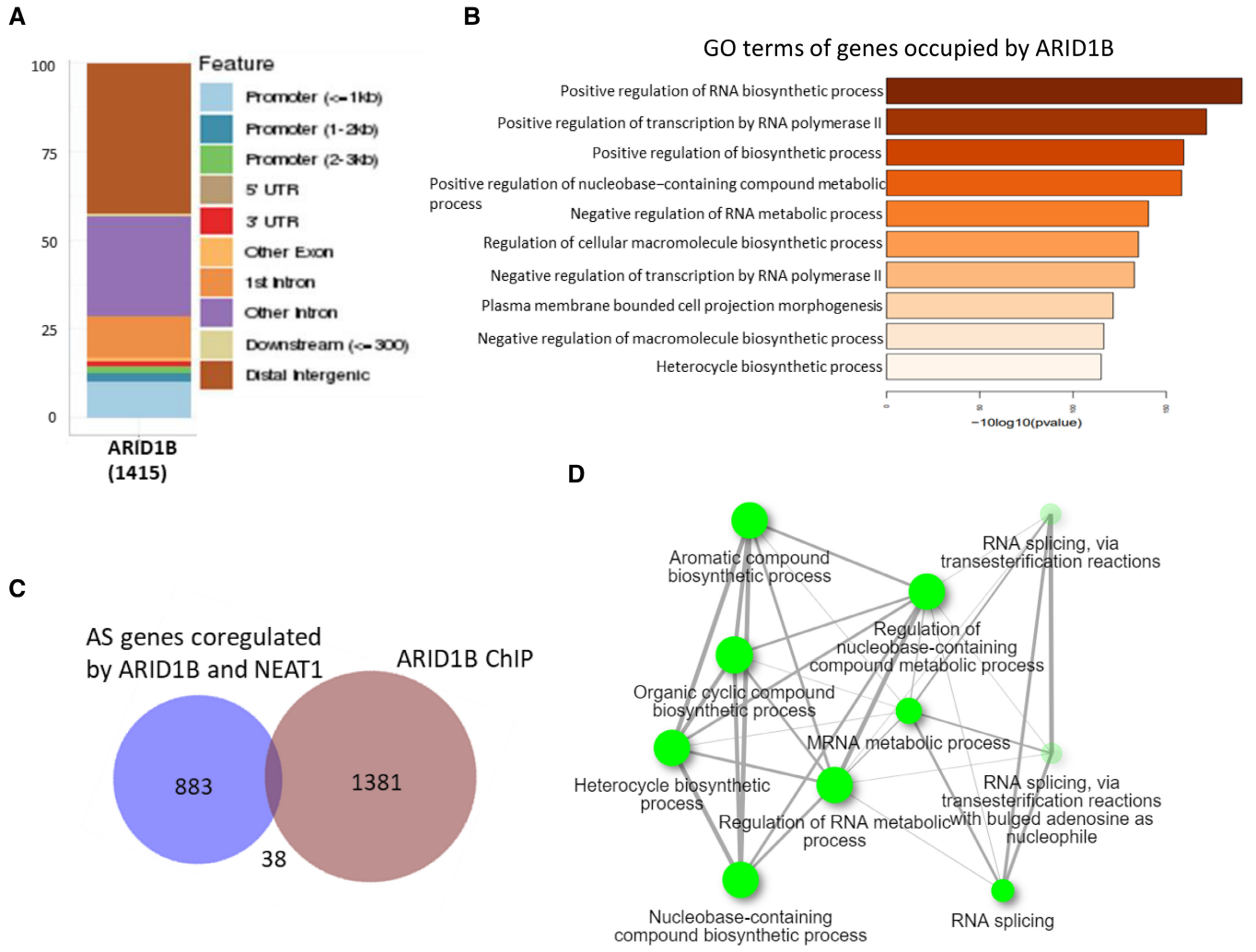

Figure EV5. ARID1B predominantly localizes near introns and distal intergenic regions.

A Graph showing the annotation and genomic distribution analysis of the ARID1B ChIP peaks.
B GO analysis of the genes occupied with ARID1B.
C Venn diagram depicting the overlap between AS changes coregulated by ARID1B/NEAT1 and the ARID1B ChIP genes.
D Pathway analysis performed for the 38 overlapping genes identified as coregulated by ARID1B/NEAT1 and occupied by ARID1B.